

Effect of Exchange Interaction on Spin Dephasing in a Double Quantum Dot

E. A. Laird,¹ J. R. Petta,¹ A. C. Johnson,¹ C. M. Marcus,¹ A. Yacoby,² M. P. Hanson,³ and A. C. Gossard³

¹Department of Physics, Harvard University, Cambridge, Massachusetts 02138, USA

²Department of Condensed Matter Physics, Weizmann Institute of Science, Rehovot 76100, Israel

³Materials Department, University of California at Santa Barbara, Santa Barbara, California 93106, USA

(Dated: 2 February 2006)

We measure singlet-triplet dephasing in a two-electron double quantum dot in the presence of an exchange interaction which can be electrically tuned from much smaller to much larger than the hyperfine energy. Saturation of dephasing and damped oscillations of the spin correlator as a function of time are observed when the two interaction strengths are comparable. Both features of the data are compared with predictions from a quasistatic model of the hyperfine field.

Implementing quantum information processing in solid-state circuitry is an enticing experimental goal, offering the possibility of tunable device parameters and straightforward scaling. However, any realization will require control over the strong environmental decoherence typical of solid-state systems. An attractive candidate system uses electron spin as the holder of quantum information [1, 2]. In III-V semiconductor quantum dots, where the highest degree of spin control has been achieved [3, 4, 5, 6, 7, 8, 9], the dominant source of decoherence is due to the hyperfine interaction with the lattice nuclei [10]. A recent experiment [9] studied this decoherence in a qubit encoded in a pair of spins [11]. In this situation, the dynamics are governed by two competing effects: the hyperfine interaction, which tends to mix the singlet and triplet basis states, and exchange, which tends to preserve them.

The interplay of hyperfine and exchange effects has been studied recently via spin-blockaded transport in two double-dot systems [12, 13]. Suppression of mixing [13] as well as oscillations [12] and bistability [13] of the leakage current were observed. The topic also has a long history in physical chemistry: recombination of a radical pair created in a triplet state proceeds significantly faster for radicals containing isotopes whose nuclei carry spin [14]. By lifting the singlet-triplet degeneracy, the exchange interaction suppresses spin transitions; its strength can be deduced from the magnetic field dependence of the recombination rate [15]. However, exchange is difficult to tune *in situ* in chemical systems.

In this Letter, singlet correlations between two separated electrons in a GaAs double dot system are measured as a function of a gate-voltage tunable exchange J and as a function of time following the preparation of an initial singlet. This study gives insight into the interplay of local hyperfine interactions and exchange in a highly controllable quantum system. Specifically, we measure the probability $P_S(\tau_S)$ that an initial singlet will be detected as a singlet after time τ_S for J ranging from much smaller than to much greater than the rms hyperfine interaction strength in each dot, E_{nuc} . When $J \ll E_{\text{nuc}}$, we find that P_S decays on a timescale $T_2^* \sim 15$ ns. In the

opposite limit where exchange dominates, $J \gg E_{\text{nuc}}$, we find that singlet correlations are substantially preserved over hundreds of ns. In the intermediate regime, where $J \sim E_{\text{nuc}}$, we observe oscillations in P_S that depend on the ratio E_{nuc}/J . Our results show that a finite exchange energy can be used to extend spin correlations for times well beyond T_2^* .

These observations are in reasonable agreement with recent theory, which predicts a singlet probability (assuming perfect readout) $P_S^0(\tau_S)$ that exhibits damped oscillations as a function of time and a long-time saturation that depends solely on the ratio E_{nuc}/J [16]. To compare experiment and theory quantitatively we introducing an empirical visibility, V , to account for readout

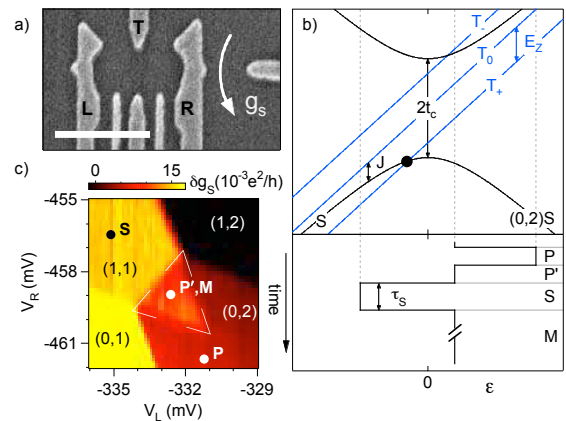


FIG. 1: (Color online) (a) Micrograph of a device with the same gate design as the one measured (Scale bar = 500 nm.) Voltages applied to gates L and R are used to adjust the detuning ϵ of the double dot; voltage applied to gate T sets the tunnel coupling between dots. The conductance g_s of a sensor quantum point contact on the right monitors the average occupation of each dot. (b) Upper panel: Level diagram for the double dot near the (1,1)-(0,2) transition ($\epsilon = 0$) plotted versus detuning ϵ . Exchange (J) and Zeeman (E_Z) energies are indicated. • denotes the S-T₊ degeneracy. Labels (m, n) denote the occupancies of the left and right dot respectively. Lower panel: The prepare (P, P') - separate (S) - measure (M) pulse scheme. ~90% of the cycle is spent in M. (c) Charge sensor conductance close to the (1,1)-(0,2) transition during application of pulses, showing the pulse triangle (marked) and the positions of points P, P', S and M. A background plane has been subtracted.

inefficiency, $P_S(\tau_S) = 1 - V(1 - P_S^0(\tau_S))$.

The device used in the experiment, shown in Fig. 1(a), is fabricated on a GaAs/Al_{0.3}Ga_{0.7}As heterostructure with a two-dimensional electron gas (density $2 \times 10^{15} \text{ m}^{-2}$, mobility $20 \text{ m}^2/\text{Vs}$) 100 nm below the surface. Ti/Au top gates define a double quantum dot in which each dot can be tuned from zero to several electrons. The inter-dot tunnel coupling t_c and (0,2)-(1,1) detuning ϵ are also separately tunable. A charge-sensing quantum point contact with conductance $g_s \sim 0.2e^2/h$ allows the occupancy of each dot to be separately measured [17, 18]. We monitor g_s using a lock-in amplifier with a 1 nA current bias at 335 Hz, with a 30 ms time constant.

Measurements were made in a dilution refrigerator at base electron temperature $T_e \approx 100 \text{ mK}$ measured from the width of the (1,1)-(0,2) transition [19]. Gates L and R (see Fig. 1) were connected via filtered coaxial lines to the output channels of a Tektronix AWG520. We report measurements for two settings of tunneling strength, controlled using voltages on gate T and measured from the width of the (1,1)-(0,2) transition: $t_c \approx 23 \mu\text{eV}$ (“large t_c ”) and $t_c < 9 \mu\text{eV}$ (“small t_c ”) [19]. Except where otherwise stated, all measurements were taken in a perpendicular magnetic field of 200 mT, corresponding to a Zeeman energy $E_Z = 5 \mu\text{eV} \gg E_{\text{nuc}}$.

Figure 1(b) shows schematically the relevant energy levels near the (1,1)-(0,2) charge transition, where measurements are carried out, as a function of energy detuning ϵ between these two charge states. In the absence of tunnel coupling, the (1,1) singlet S and $m_s = 0$ triplet T₀ are degenerate; the $m_s = \pm 1$ triplets T_± are split off in energy from T₀ by $\mp E_Z$. Finite t_c leads to hybridization of the (0,2) and (1,1) singlets, inducing an exchange splitting J between S and T₀. The (0,2) triplet (not shown) is split off by the much larger intra-dot exchange energy $J_{(0,2)} \sim 600 \mu\text{eV}$ [20] and is inaccessible. Rapid mixing due to hyperfine interaction occurs between states whose energies differ by less than E_{nuc} . In the present configuration, this occurs at large negative ϵ (lower left of Fig. 1(b)), where S and T₀ mix, and at $J(\epsilon) = E_Z$ (black dot in Fig. 1(b)), where S and T₊ mix.

A cycle of gate configurations is used to prepare and measure two-electron spin states in the {S, T₀} basis [9], as illustrated in Fig. 1(b). A 200 ns preparation step (denoted P in Fig. 1) configures the dot in (0,2) at a position where the series (0,2)T₀→(0,1)→(0,2)S is energetically allowed and occurs rapidly, giving efficient initialization to a singlet. The gates then shift (waiting 200 ns at P' to reduce pulse overshoot) to a separation point (S) in (1,1) for a time τ_S during which singlet-triplet evolution occurs. Finally, the gates are set to the measurement point (M) for $\tau_M = 5 \mu\text{s}$, providing a spin-state to charge conversion. Inside the pulse triangle marked in Fig. 1(c), the triplet states will remain in (1,1) over the measurement time τ_M [8, 21]. Since $\sim 90\%$ of the pulse cycle is spent at M, the relatively slow measurement of the sensor

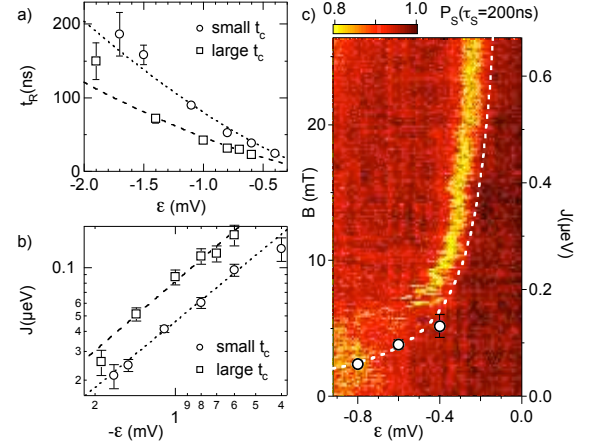


FIG. 2: (Color online) (a) Period t_R of first Rabi oscillation versus exchange point detuning for small and large tunnel coupling. (b) Exchange energy as a function of detuning, deduced from the data in (a), together with empirical power-law fits $J \propto |\epsilon|^{-1.4 \pm 0.1}$. t_R corresponding to the fits is shown as curves in (a). (c) Comparison (for small t_c) of exchange energy deduced from Rabi oscillations and from S-T₊ degeneracy location. Points: data in (b). Curve: fit from (b). Color plot: Singlet probability as a function of S-point detuning and magnetic field in the pulse scheme of Fig. 1(b). The bright band indicates rapid decoherence where $J \approx |g|\mu_B B$, where μ_B is the Bohr magneton. The two methods give a consistent $J(\epsilon)$. The same agreement is seen in the data for large t_c (not shown).

g_s gives a time-averaged charge configuration at the M point. The time-averaged g_s signal is calibrated to give a singlet state probability $P_S(\tau_S)$ by comparing the signal in the pulse triangle with the values measured in the (1,1) and (0,2) regions of the charge stability diagram. When the gates are configured so that M is outside the pulse triangle in (0,2), both singlet and triplet relax rapidly to (0,2); g_s in this region defines $P_S = 1$. When M is in (1,1), the value of g_s defines $P_S = 0$.

We first measure $J(\epsilon)$, E_{nuc} , and V at two values of t_c , allowing the saturation probability $P_S(\infty)$ to be measured as a function of J . Here we find good agreement with theory [16], including the predicted dependence of $P_S(\infty)$ on the ratio E_{nuc}/J . We then measure the time evolution $P_S(\tau_S)$, which shows damped oscillations, also in reasonable agreement with theory [16]. $J(\epsilon)$ is measured by two methods. In the first – the Rabi (or Larmor) sequence described in Ref. [9] – an adiabatic (compared with E_{nuc}) ramp over 1 μs to (1,1) is used to prepare and measure the electron spin state in the $\{|\uparrow\downarrow\rangle, |\downarrow\uparrow\rangle\}$ basis. An exchange pulse produces coherent rotations with a period t_R (shown in Fig. 2(a)) from which we deduce the exchange coupling $J(\epsilon) = h/t_R$ [22]. Values of $J(\epsilon)$ for small and large t_c are shown in Fig. 2(b), along with a fit to an empirical power-law form $J \propto \epsilon^{-\alpha}$, giving $\alpha \sim 1.4$ [23]. In the second method, rapid dephasing at the S-T₊ degeneracy appears as a dip in P_S when the value of ϵ at the S point satisfies $J(\epsilon) = E_Z$. $J(\epsilon)$ can then be measured from a knowledge of the field, using $E_Z = g\mu_B B$, and taking the value $g = -0.44$, measured in a different

quantum dot device on made from the same wafer [24]. The two methods yield consistent measurements of $J(\epsilon)$, as seen in Fig. 2.

Parameters E_{nuc} and V are extracted from $P_S(\tau_S)$ measured for the S-point at large negative ϵ , where $J \ll E_{\text{nuc}}$. In this regime the initial singlet evolves into an equal mixture of singlet and triplet with characteristic time h/E_{nuc} . $P_S(\tau_S)$ for small and large t_c (shown in the insets of Fig. 3) are fit to the form for $P_S^0(\tau_S)$ given in [16], with fit parameters $E_{\text{nuc}} = 45 \pm 3$ neV (47 ± 4 neV) and $V = 0.53 \pm 0.02$ (0.46 ± 0.02) for small (large) t_c . These hyperfine energies correspond to an effective hyperfine field of 1.8 mT, similar to the value measured previously on this device [9]. The function $P_S^0(\tau_S)$ incorporates a value of $J(\epsilon)$ extrapolated from Fig. 2; however, since J is so small at this large $|\epsilon|$, the best-fit parameters are essentially independent of details of the extrapolation, and, for example, are within the error bars even for $J = 0$.

The variance of the hyperfine field arises either from a quantum superposition of nuclear-field eigenstates or through dynamics of the nuclear system on timescales faster than the measurement averaging time [16]. $P_S^0(\tau_S)$ is calculated by integrating Schrödinger's equation from the initial singlet for given nuclear fields and then averaging the resulting singlet probability over nuclear fields. The resulting $P_S^0(\tau_S)$ shows a range of interesting behavior depending on the relative magnitudes of J and E_{nuc} [16]: In the limit $J = 0$, $P_S^0(\tau_S \rightarrow \infty)$ rapidly saturates to 1/2. As J is increased, hyperfine dephasing becomes less effective, with $P_S^0(\infty)$ saturating at progressively higher values, approaching unity when $J \gg E_{\text{nuc}}$, and following a universal function of E_{nuc}/J . As a function of τ_S , $P_S^0(\tau_S)$ is predicted to undergo damped oscillations, which when plotted versus $\tau_S J$ follow another universal function of E_{nuc}/J and exhibit a universal phase shift of $3\pi/4$ at large $\tau_S J$.

Knowing $J(\epsilon)$ and E_{nuc} allows the long-time ($\tau_S \gg h/J$) saturation of the measured P_S to be compared with theory [16]. We set $\tau_S = 400$ ns and sweep the position of the S-point. For small and large t_c , $P_S(400 \text{ ns})$ is plotted in Fig. 3 as a function of E_{nuc}/J , where E_{nuc} is obtained from the fits described above and $J(\epsilon)$ are taken from Fig. 2. At the most negative detunings (in the regions marked by gray bars in Fig. 3) J is too small to be measured by either Rabi period or S-T₊ degeneracy methods; instead, $J(\epsilon)$ is found by extrapolating the power-law fits (Fig. 2.) The quality of these fits over more than an order of magnitude of measured $J(\epsilon)$ gives some confidence in the extrapolation; in any case, agreement with theory (discussed below) is insensitive to the details of the extrapolation.

The long- τ_S P_S data shown in Fig. 3 agrees fairly well with the saturation values predicted from [16], taking into account the visibility obtained from the insets. In particular, P_S has the same dependence on E_{nuc}/J at both values of t_c measured, even though the function $J(\epsilon)$ de-

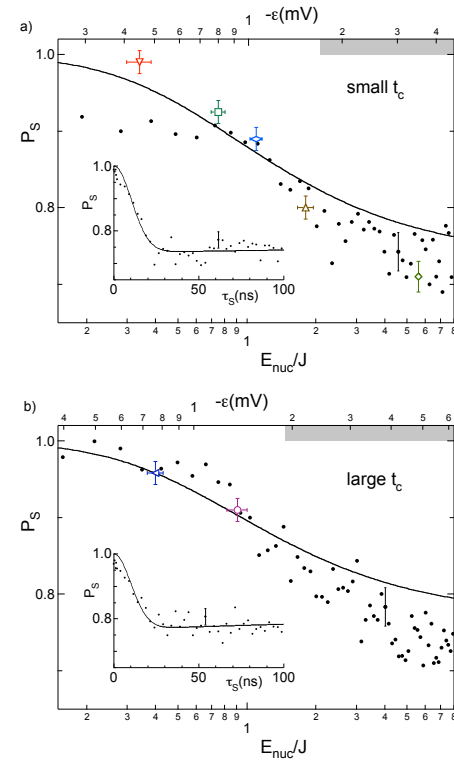


FIG. 3: (Color online) (a) Inset: Singlet probability $P_S(\tau_S)$ for small t_c and $\epsilon = -5.5$ mV, with fit (see text) giving $E_{\text{nuc}} = 45 \pm 3$ neV and $V = 0.53 \pm 0.02$. Main panel: Measured $P_S(\tau_S = 400 \text{ ns})$ (points) plotted against E_{nuc}/J . Open symbols correspond to P_S in the traces of Fig. 4(a) at the largest τ_S measured for each ϵ . Curve shows theoretical dependence (from [16]) of $P_S(\tau_S \rightarrow \infty)$ on E_{nuc}/J , taking into account the measurement fidelity deduced from the inset. The gray bar along the top axis indicates the region where $J(\epsilon)$ is extrapolated (see text). (b) The same data for large t_c . The corresponding fit to the inset gives $E_{\text{nuc}} = 47 \pm 4$ neV and $V = 0.46 \pm 0.02$, from which the theoretical saturation P_S (curve in main panel) is calculated. Open symbols correspond to the large- τ_S values in Fig. 4(b).

pends on t_c . P_S is slightly smaller than expected from theory; this could be due to cotunneling or nuclear decorrelation over the duration of the separation pulse, both of which tend to equalize singlet and triplet occupations.

We next investigate the time dependence of $P_S(\tau_S)$ at finite J . For five S-point detunings at small t_c and two detunings at large t_c , $P_S(\tau_S)$ was measured out to $\tau_S J/\hbar \approx 15$. The results are shown in Fig. 4, together with the predicted time evolution from [16] with values for V and E_{nuc} taken from fits shown in the insets of Fig. 3. Because P_S remains close to unity, these data are particularly sensitive to calibration imperfections caused by quantum point contact nonlinearities and noise in the calibration data, whose effect to lowest order is to shift the data vertically. Traces in Fig. 4 are therefore shifted vertically to satisfy the constraint $P_S(\tau_S = 0) = 1$. In no case was this greater than ± 0.05 . (There is, in addition, a trivial offset of data and theory for clarity.)

Damped oscillations are observed as predicted in [16];

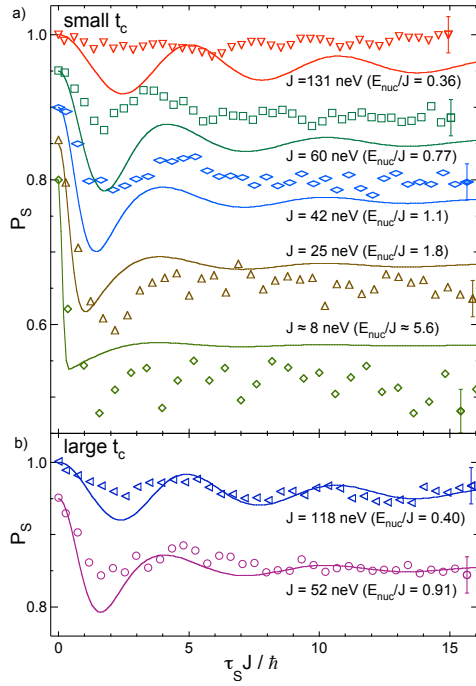


FIG. 4: (Color online) (a) Symbols: Experimental $P_S(\tau_S)$ at small t_c for various J , plotted as a function of $\tau_S J / \hbar$. Curves: Predictions from [16] using E_{nuc} and V fit from Fig. 3(a). Adjacent traces after the topmost are offset by 0.05 for clarity. (b) Corresponding data for large t_c . Lower trace is offset by 0.05 for clarity.

however, even after taking account the empirical visibility factor, the amplitude of the oscillations is less than expected. This is likely due to the finite rise time of the separation pulse and to switching noise, which make each trace effectively an average over a range of J values. The period and phase of the oscillations approximately match the predictions of [16], although the expected shift in the position of the first valley to smaller $\tau_S J$ is not observed at intermediate J . Similar oscillations of P_S are predicted close to the S-T₊ degeneracy with a characteristic frequency $\sim \Delta = J - E_Z$. We have searched for these oscillations but do not observe them. We believe the reason for this is that Δ varies much more rapidly with ϵ in this region than J does at the S-T₀ near-degeneracy; the oscillations are therefore washed out by switching noise and pulse overshoot.

In summary, after including the measured readout efficiency, we find that spin dephasing in a two-electron system with competing exchange and hyperfine interactions is in reasonable quantitative agreement with theory [16] using a single parameter across the whole range $J \gg E_{\text{nuc}}$ to $J \ll E_{\text{nuc}}$. The singlet probability undergoes damped

oscillations as function of time, with roughly the expected period and phase, and saturates as predicted at a value that depends only on E_{nuc}/J . Departures from expected behavior can be explained by cotunneling, nuclear decorrelation, and device noise.

We acknowledge useful discussions with W. Coish, H. A. Engel, D. Loss, M. Lukin, J. M. Taylor. This work was supported by DARPA-QuIST and the ARO/ARDA STIC program.

- [1] D. Loss and D. P. DiVincenzo, Phys. Rev. A **57**, 120 (1998).
- [2] J. M. Taylor *et al.*, Nature Physics **1**, 177 (2005).
- [3] T. Fujisawa *et al.*, Nature **419**, 278 (2002).
- [4] J. M. Elzerman *et al.*, Nature **430**, 431 (2004).
- [5] A. S. Bracker *et al.*, Phys. Rev. Lett. **94**, 047402 (2005).
- [6] P.-F. Braun *et al.*, Phys. Rev. Lett. **94**, 116601 (2005).
- [7] R. Hanson *et al.*, Phys. Rev. Lett. **94**, 196802 (2005).
- [8] A. C. Johnson *et al.*, Nature **435**, 925 (2005).
- [9] J. R. Petta *et al.*, Science **309**, 2180 (2005).
- [10] S. I. Erlingsson, Y. V. Nazarov, V. I. Fal'ko, Phys. Rev. B **64**, 195306 (2001); I. A. Merkulov, A. L. Efros, and M. Rosen, Phys. Rev. B **65**, 205309 (2002); A. V. Khaetskii, D. Loss, and L. Glazman, Phys. Rev. Lett. **88**, 186802 (2002).
- [11] J. Levy, Phys. Rev. Lett. **89**, 147902 (2002).
- [12] K. Ono and S. Tarucha, Phys. Rev. Lett. **92**, 256803 (2004).
- [13] F. H. L. Koppens *et al.*, Science **309**, 1376 (2005).
- [14] Reviewed in: Nicholas J. Turro, Proc. Nat. Acad. Sci. **80**, 609 (1983); A. L. Buchachenko, J. Phys. Chem. A **105**, 9995 (2001).
- [15] H. Staerk *et al.*, Chem. Phys. Lett. **118**, 19 (1985); V. F. Tarasov *et al.*, J. Am. Chem. Soc. **114**, 9517 (1992).
- [16] W. A. Coish and D. Loss, Phys. Rev. B **72**, 125337 (2005).
- [17] M. Field *et al.*, Phys. Rev. Lett. **70**, 1311 (1993).
- [18] J. M. Elzerman *et al.*, Phys. Rev. B **67**, 161308 (2003).
- [19] L. DiCarlo *et al.*, Phys. Rev. Lett. **92**, 226801 (2004).
- [20] A. C. Johnson *et al.*, Phys. Rev. B **72**, 165308 (2005).
- [21] J. R. Petta *et al.*, Phys. Rev. B **72**, R161301 (2005).
- [22] When $J \lesssim E_{\text{nuc}}$, J must be corrected downwards slightly because precession in the nuclear field enhances the average Rabi frequency. We calculate the size of the correction by solving Schrödinger's equation during the exchange pulse and averaging numerically over nuclear field configurations. In no case does the correction to J exceed 13 %.
- [23] A simple level anticrossing with t_c and ϵ independent would give $J \propto \epsilon^{-1}$. The discrepancy may be due to a detuning-dependent t_c .
- [24] D. M. Zumbühl *et al.*, Phys. Rev. Lett. **93**, 256801 (2004).